Growth laws for channel networks incised by groundwater flow

Daniel M. Abrams[1], Alexander E. Lobkovsky[2], Alexander P. Petroff[1], Kyle M. Straub[3], Brandon McElroy[4], David C. Mohrig[4], Arshad Kudrolli[5], and Daniel H. Rothman[1]

[1]*Department of Earth, Atmospheric and Planetary Sciences, Massachusetts Institute of Technology, Cambridge, MA 02139 USA*
[2]*Department of Physics, Georgetown University, Washington, D.C. 20057 USA*
[3]*Department of Earth and Environmental Sciences, Tulane University, New Orleans, LA 70118 USA*
[4]*Department of Geological Sciences, University of Texas at Austin, Austin, TX 78712 USA*
[5]*Department of Physics, Clark University, Worcester, MA 01610 USA*

July 21, 2008

Wherever infiltration exceeds rainfall, runoff must travel at least partially underground. The reemergence of groundwater at the surface can then shape topography by a process called seepage erosion[1–5]. Along with overland flow[6], seepage erosion contributes to the initiation and growth of channel networks[1–5]. Because seepage processes undermine overlying material, they have been been suggested as an explanation of enigmatic amphitheater-headed channel networks on Earth[7–11] and Mars[12–14]. Nevertheless, the role of seepage in producing such channels remains controversial[11,15,16]. Progress requires relating mechanisms of growth to geologic form. By combining field observations with physical theory, here we show that two simple linear response relations suffice to characterize key aspects of the growth and form of a kilometer-scale seepage-driven channel network in the Florida Panhandle[17]. The first growth law states that the velocity at which channel heads advance is proportional to the flux of groundwater to the heads[18]. The second states that tip-splitting and side-branching events occur at a rate proportional to the total groundwater flux drained by the network. We

show that the dynamics defined by the first growth law is reversible, and use this remarkable property to reconstruct the history of network growth and estimate its age. Developed networks exhibit a characteristic length scale between channels[19]. Our theory predicts the evolution of this length scale, thereby linking network growth dynamics to geometric form.

Networks of amphitheater-headed channels known as "steephead streams"[17] occur abundantly in Liberty County, Florida, east of the Apalachicola River on the Florida Panhandle (Fig. 1). The steepheads are incised into 65 meters of laterally persistent, medium to coarse, fluviodeltaic and marine sands of Late Pliocene to Pleistocene origin[20], deposited during progradation of the Apalachicola delta[21]. These sands unconformably overlie 15 meters of muddy Miocene marine carbonates and sands[20]. Steephead springs occur in the Late Pliocene to Pleistocene sands and examination of the deposit at spring sites reveals no obvious stratigraphic control on their vertical positions[17].

To investigate controls on the horizontal position of springs, we conducted a three-dimensional ground-penetrating radar survey of the water table near a highly bifurcated segment of the channel network. (See Supplementary Information.) Figure 2a shows that the water table descends as much as 6 m from its highest point midway between channels before reaching the outer contour of the channel network. In general, the height of the water table is a complex function of the spatial distribution of sources (i.e., rainfall), sinks (the channel network), and subsurface heterogeneities[22,23]. Because rainfall is uniform at this scale, we can test for the influence of heterogeneities by plotting water table height vs. the distance to the nearest channel. The good correlation shown in Figure 2b suggests that distance to the nearest channel, rather than heterogeneities, is the primary deter-

minant of the water table's shape. Consequently the location of springs and the regular structure of this branched drainage network must be a consequence of the intrinsic dynamics of subsurface flow, seepage erosion, and sediment transport.

The correlation of Figure 2b also suggests that the flux of water into any location on the channel should be proportional to the planform area that is closer to that location than to any other. We call this area the *geometric drainage area* and plot it in Figure 3a for each channel tip in the network. Numerical solution of the full three-dimensional hydrodynamic equations for groundwater flow shows that this geometric construction well approximates the relative flux to the tips of channels of varying length. (See Supplementary Information.)

Howard[18] suggested that the headward erosion rate of a channel tip is proportional to the groundwater flux to the tip. Approximating the flux into the ith tip by the rainfall per unit time into the geometric drainage area a_i associated with that tip then suggests that tip velocity v_i scales like

$$v_i = \beta a_i, \tag{1}$$

where β is a transport coefficient (assumed constant) with units $(LT)^{-1}$.

If equation (1) is correct, fast-moving channel tips should be associated with large geometric drainage areas. Figure 3b suggests additionally that larger areas are associated with sharper corners as longitudinal channel profiles rise toward the relatively flat plain at the channel lip. This relation between curvature and area may be understood by assuming that a steady-state channel profile results from a balance between the average erosion rate due to advection and that due to diffusion. Mathematically, this means $\langle \vec{u} \cdot \nabla h \rangle \sim \langle D \nabla^2 h \rangle$, where h is elevation, D is the topographic diffusivity[24] (assumed constant), $\vec{u}$ is the horizontal velocity of an elevation contour,

and the angle brackets represent averaging over the channel head. Restricting our attention to the longitudinal profile then yields $v \sim D/r$, where r is a characteristic length scale that varies from channel to channel in response to changes in the headward velocity v. We identify r with the radius of curvature of the channel lip. We then test equation (1) by asking whether the curvature r^{-1} increases linearly with area. Figure 3c demonstrates that the data is indeed consistent with $r^{-1} \simeq \beta a/D$, thereby validating (1) and providing an estimate of β/D. Noting that the median radius of curvature is 66 m and assuming that the diffusivity $D \simeq 0.02$ m^2/yr [25–28], we find that the headward velocity $v \sim D/r \sim 0.3$ mm/yr, consistent with a previous estimate[17].

The water table's shape adjusts continually in response to the advance of channel tips. Given the typical hydraulic conductivity $K \sim 10^{-3}$ m/s for sand[23] and a typical tip-area $a \sim 4 \times 10^4$ m^2, the time scale for relaxation of the water table is $\sqrt{a}/K \sim 2$ days. Consequently the water table adjusts rapidly—i.e., *quasistatically*—on the time scale of headward growth.

This mundane observation has a profound implication: the headward growth described by equation (1) is reversible. We therefore evolve the network backwards in time by retracting tips i at velocity $-\beta a_i$, continuously updating the a_i's as the network geometry changes. Reversing the process yet again so that time marches forward then provides a reconstruction of the network's growth. Figure 4 shows that new channel tips are generated by both side-branching and tip-splitting events. Computer animation (see Supplementary Information) reveals the process dynamically.

An immediate consequence of the reconstruction is an ability to estimate the age of the network. Letting ℓ be the length of a stream and t the time it takes to grow with time-averaged tip

velocity $\bar{v}$ and tip area $\bar{a}$, we have

$$t = \frac{\ell}{\bar{v}} = \frac{\ell}{\beta \bar{a}} = \frac{1}{D}\left(\frac{D}{\beta}\right)\left(\frac{\ell}{\bar{a}}\right), \tag{2}$$

where the second equality follows from averaging equation (1). For the longest channel of the modern network, $\ell \simeq 3.9 \times 10^3$ m and $\bar{a} \simeq 8.3 \times 10^5$ m^2. Using our previous estimate[25–28] of the diffusivity D and our estimate of D/β from Figure 3c then yields $t \simeq 0.73$ Myr, roughly accurate within a factor of two, and consistent with the Plio-Pleistocene age ($\sim$2 Myr) of the sand. These numbers imply that the time-averaged tip velocity is about 5.3 mm/yr. Averaging over all channels for the last 10,000 yr of the network's evolution, however, reveals that the current network is growing more slowly, at about 0.5 mm/yr, which represents a refinement of our previous estimate using channel curvature.

More fundamentally, the reconstruction also reveals an approximate rate law for the generation of new channels by tip-splitting and side-branching. Let $A(t)$ equal the total area drained by the network. Then $\dot{N}/L$ is the production rate, per unit length, of new tips, and A/L is the drainage area, per unit length, into the entire network. The generation of new channel tips must ultimately derive from an erosional instability[1–5,29,30]. We know of no theory for this instability, but the mechanism that drives it must be drainage into the network. Consequently we expect that A/L is proportional to a force density that creates new tips at rate $\dot{N}/L$ per unit length. Hypothesizing a linear response, we obtain

$$\frac{\mathrm{d}N}{\mathrm{d}t} = \alpha A, \tag{3}$$

where α is a rate constant per unit area, with units $(L^2T)^{-1}$. We test the integral form of (3) by plotting $N(t)$, the number of channel tips, versus $\int_0^t A(t')dt'$. The result, shown in the inset of

Figure 4, is consistent with the linear response (3); the slope gives the rate constant α.

The linear response relations (1) and (3) provide, respectively, the growth and birth rates of channels. The ratio of the transport coefficient β to the rate constant α is a length scale that represents the characteristic growth of the network's total length L during the characteristic time between the birth of new channels. We can obtain β/α explicitly by noting from (1) that $\dot{L} = \beta \sum_i a_i$ and integrating to obtain $\beta t = L/\sum_i \bar{a}_i$. On the other hand, integration of equation (3) yields $\alpha t = N/\bar{A}$, where $\bar{A}$ is the time-averaged area draining into the entire network. Then

$$\frac{\beta}{\alpha} = \frac{L(t)}{N(t)} \left(\frac{\bar{A}(t)}{\sum_i \bar{a}_i(t)} \right). \tag{4}$$

Note that all terms on the right-hand side depend on time, but the left-hand side does not. Thus lengths, areas, and the number of channels must evolve such that β/α is constant. Our reconstruction confirms this prediction: over the last half of the network's growth, $\beta/\alpha \simeq 461$ m with a root-mean square fluctuation of less than 3%.

To further understand the length scale β/α, we define the dimensionless "screening efficiency" $S = \sum_i \bar{a}_i/\bar{A}$. Substitution into (4) and rearranging then yields

$$L = \left(\frac{\beta}{\alpha} \right) SN. \tag{5}$$

The screening efficiency $0 \leq S \leq 1$ is the fractional extent to which tips draw groundwater away from channel sidewalls. In the limit in which all groundwater flows to tips, $S = 1$ and each tip contributes a length β/α to the total channel length L, consistent with our dimensional argument. Less efficient screening ($S < 1$) implies less length per tip. (Here we find $S = 0.59 \pm 0.01$ while $\beta/\alpha \simeq$ const.) But the fundamental length scale that must determine all other lengths is β/α.

Foremost among network length scales is the average distance A/L between any point on the network and the closest groundwater divide. This "dissection" scale[19] is the inverse of Horton's drainage density[6] L/A, which is readily obtained by dividing both sides of (5) by A. One sees immediately that the drainage density increases as the number N of tips grows.

Decades ago, Dunne[1,3,4] advanced a conceptual model for the development of seepage-driven networks. Its principal components—headward growth due to groundwater focusing and generation of new channel heads by tip-splitting and side-branching—are encoded here in terms of two linear response relations. After validating these linear laws by analysis of the Florida network's present and past development, we find that the evolution of lengths, drainage density, and number of tips is slaved to the transport coefficient β and rate constant α that set the respective time scales for the network's growth and ramification. This result provides an explicit link between the dynamics of a network and its static structure. Although this link does not by itself provide an immediate method for resolving the mysterious provenance of other amphitheater-headed channels[7–16], we expect that the growth laws upon which it is based will be useful for understanding the mechanisms that produce such shapes in addition to providing further reconstructions of past network growth.

References

1. Dunne, T. *Runoff production in a humid area*. Ph.D. thesis, Johns Hopkins University (1969). Also published as U.S. Deparment of Agriculture Report ARS 41-160 (1970).

2. Dunne, T. Field studies of hillslope flow processes. In Kirkby, M. J. (ed.) *Hillslope Hydrology*, 227–293 (Wiley, Chichester, 1978).

3. Dunne, T. Formation and controls of channel networks. *Progress in Physical Geography* **4**, 211–239 (1980).

4. Dunne, T. Hydrology, mechanics, and geomorphic implications of erosion by subsurface flow. In Higgins, C. G. & Coates, D. R. (eds.) *Groundwater geomorphology; the role of subsurface water in Earth-surface processes and landforms*, Geological Society of America Special Paper 252, 1–28 (Geological Society of America, Boulder, CO, 1990).

5. Dietrich, W. E. & Dunne, T. The channel head. In Beven, K. & Kirby, M. J. (eds.) *Channel Network Hydrology*, 175–219 (John Wiley and Sons Ltd, New York, 1993).

6. Horton, R. E. Erosional development of streams and their drainage basins; hydrophysical approach to quantitative morphology. *Geological Society of America Bulletin* **56**, 275–370 (1945).

7. Wentworth, C. K. Principles of stream erosion in Hawaii. *Journal of Geology* **36**, 385–410 (1928).

8. Laity, J. E. & Malin, M. C. Sapping processes and the development of theater-headed valley networks on the Colorado plateau. *Geol. Soc. Am. Bull.* **96**, 203–17 (1985).

9. Orange, D. L., Anderson, R. S. & Breen, N. A. Regular canyon spacing in the submarine environment: the link between hydrology and geomorphology. *GSA Today* **4**, 1–39 (1994).

10. Schorghofer, N., Jensen, B., Kudrolli, A. & Rothman, D. H. Spontaneous channelization in permeable ground: Theory, experiment, and observation. *Journal of Fluid Mechanics* **503**, 357–374 (2004).

11. Lamb, M. P. *et al.* Can springs cut canyons into rock? *Journal of Geophysical Research* **111**, 18 pages (2006).

12. Higgins, C. G. Drainage systems developed by sapping on Earth and Mars. *Geology* **10**, 147–152 (1982).

13. Malin, M. C. & Carr, M. H. Groundwater formation of martian valleys. *Nature* **397**, 589–591 (1999).

14. Malin, M. C. & Edgett, K. Evidence for recent groundwater seepage and surface runoff on Mars. *Science* **288**, 2330–2335 (2000).

15. Lamb, M. P., Howard, A. D., Dietrich, W. E. & Perron, J. T. Formation of amphitheater-headed valleys by waterfall erosion after large-scale slumping on Hawaii. *GSA Bulletin* **19**, 805–822 (2007).

16. Lamb, M. P., Dietrich, W. E., Aciego, S. M., DePaolo, D. J. & Manga, M. Formation of Box Canyon, Idaho, by megaflood: Implications for seepage erosion on Earth and Mars. *Science* **320**, 1067–1070 (2008).

17. Schumm, S. A., Boyd, K. F., Wolff, C. G. & Spitz, W. J. A ground-water sapping landscape in the Florida Panhandle. *Geomophology* **12**, 281–297 (1995).

18. Howard, A. D. Groundwater sapping experiments and modelling. In Howard, A. D., Kochel, R. C. & Holt, H. E. (eds.) *Sapping Features of the Colorado Plateau, a Comparative Planetary Geology Field Guide*, 71–83 (NASA Scientific and Technical Information Division, Washington, D.C., 1988).

19. Montgomery, D. R. & Dietrich, W. E. Channel initiation and the problem of landscape scale. *Science* **255**, 826–830 (1992).

20. Schmidt, W. Alum Bluff, Liberty County, Florida. Open File Report 9, Florida Geological Survey (1985).

21. Rupert, F. R. The geomorphology and geology of Liberty County, Florida. Open File Report 43, Florida Geological Survey (1991).

22. Polubarinova-Kochina, P. I. A. *Theory of Ground Water Movement* (Princeton University Press, Princeton, NJ, 1962).

23. Bear, J. *Dynamics of Fluids in Porous Media* (Dover Publications, New York, 1972).

24. Culling, W. E. H. Analytic theory of erosion. *J. Geol.* **68**, 336–344 (1960).

25. McKean, J. A., Dietrich, W. E., Finkel, R. C., Southon, J. R. & Caffee, M. W. Quantification of soil production and downslope creep rates from cosmogenic ^{10}Be accumulations on a hillsope profile. *Geology* **21**, 343–346 (1993).

26. Rosenbloom, N. A. & Anderson, R. S. Hillslope and channel evolution in a marine terraced landscape, Santa Cruz, California. *Journal of Geophysical Research* **99**, 14,013–14,029 (1994).

27. Fernandes, N. F. & Dietrich, W. E. Hillslope evolution by diffusive processes: The time scale for equilibrium adjustments. *Water Resources Research* **33**, 1307–1318 (1997).

28. Small, E. E., Anderson, R. S. & Hancock, G. S. Estimates of the rate of regolith production using ^{10}Be and ^{26}Al from an alpine hillslope. *Geomorphology* **27**, 131–150 (1999).

29. Howard, A. D. & McLane, C. F. Erosion of cohesionless sediment by groundwater seepage. *Water Resources Research* **24**, 1659–1674 (1988).

30. Lobkovsky, A. E., Jensen, B., Kudrolli, A. & Rothman, D. H. Threshold phenomena in erosion driven by subsurface flow. *Journal of Geophysical Research-Earth Surface* **109**, Art. No. F04010, doi:10.1029/2004JF000172 (2004).

Supplementary information is linked to the online version of the paper at www.nature.com/nature.

Acknowledgements We would like to thank The Nature Conservancy for access to the Apalachicola Bluffs and Ravines Preserve, and K. Flournoy, B. Kreiter, S. Herrington, and D. Printiss for guidance on the Preserve. We would also like to thank D. Forney, D. Jerolmack, and J. T. Perron for helpful suggestions and assistance in the field. This work was supported by Department of Energy Grants FG02-99ER15004 and FG02-02ER15367.

Author contributions D.M.A., A.E.L., A.P.P., K.M.S., and D.H.R. contributed equally to this work. D.M.A., A.E.L., A.P.P., and D.H.R. developed theory and performed field work and data analysis. K.M.S. and A.K. performed field work and data analysis. B.M. and D.C.M. performed field work and analyzed regional sedimentology. D.H.R. wrote the paper, with input from D.M.A., A.E.L., A.P.P., K.M.S, and B.M.

Author information Correspondence and requests for materials should be addressed to D.H.R. (dhr@mit.edu).

Figure captions

1. Topographic map of networks of steephead channels draining into the Apalachicola River, located on the Apalachicola Bluffs and Ravines Preserve, near Bristol Florida. Topography is shaded with illumination from the east. The arrow points to the location of the water table map in Figure 2. Mapping data were collected by the National Center for Airborne Laser Mapping. The Universal Transverse Mercator coordinates run from 692000–699000 Easting and 3372000–3376000 Northing.

2. **a**, Elevation of the water table in the region indicated by the arrow in Fig. 1, along with the 35-m and 50-m elevation contour of the surface topography (black). The water table was imaged by ground-penetrating radar surveys performed along transects given by the blue lines. **b**, Elevation of the water table plotted against the shortest distance from the 35-m contour. The red curve is the best fitting Dupuit-Forchheimer ellipse[23]. The Spearman rank correlation coefficient $r = 0.69$ ($N = 1065$, $P = 0$). See Supplementary Information.

3. **a**, Backbone of the network of Fig. 1 (black) along with the geometric drainage area a (colored polygons) associated with each channel tip. Gray lines indicate boundaries used to delineate the overall basin. **b**, Longitudinal profiles of channel heads associated with small (0.01 km^2) and large (0.22 km^2) geometric drainage areas. In the former case the radius of curvature, r, is indicated. Horizontal axis is for scale only. **c**, Log-log plot of the curvature r^{-1} vs. area a for isolated non-bifurcating channel heads. The Pearson correlation coefficient $r = 0.62$ ($N = 29$, $P < 0.001$). The straight line is the best fit to $r^{-1} = (\beta/D)a$, providing the estimate $\beta/D = 3.2 \pm 0.7 \times 10^{-7}$ m^{-3}. The channel profiles of **b** correspond to the

smallest and largest areas in **c**. See Supplementary Information.

4. Reconstruction of network growth. Each colored segment corresponds to one-tenth of the elapsed time of growth. Black segments represent initial conditions. Computer animations are available in Supplementary Information. *Inset:* Plot of the number of reconstructed channel tips, N, versus $X = \int_0^\tau A(\tau')\mathrm{d}\tau'$, where $\tau = t/t_{\max}$. After an initial transient the growth is approximately linear, thereby validating equation (3).

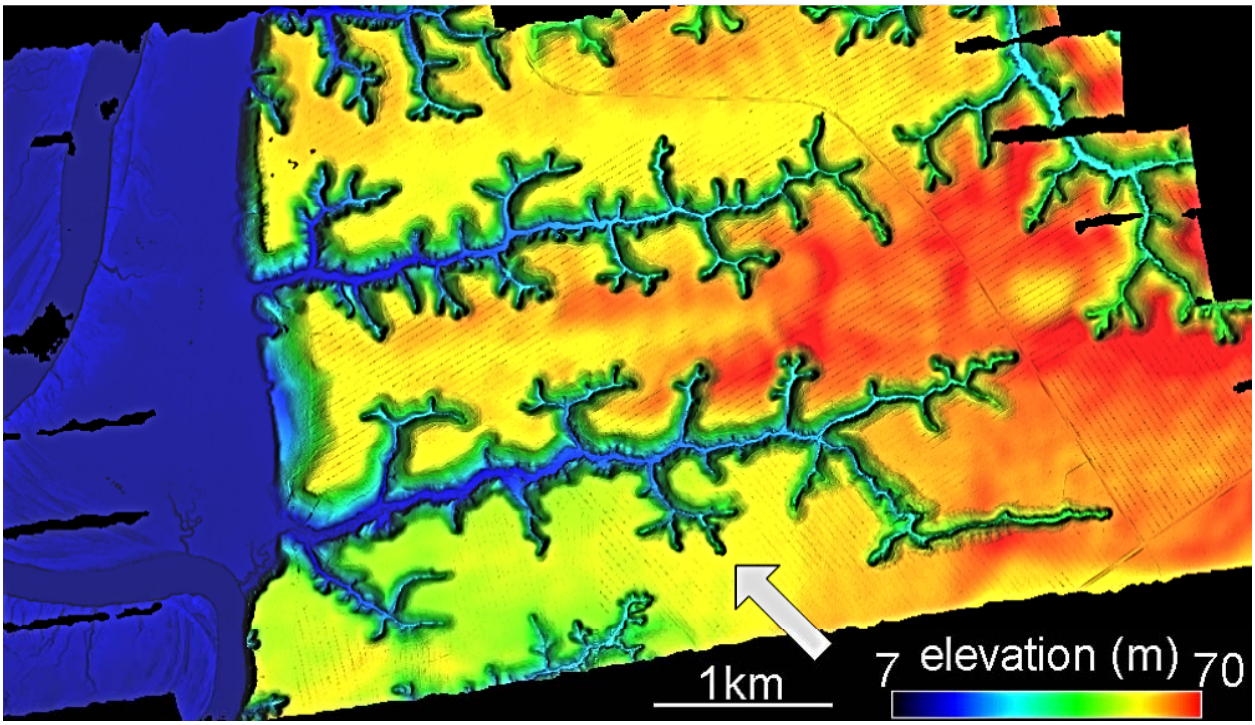

Figure 1

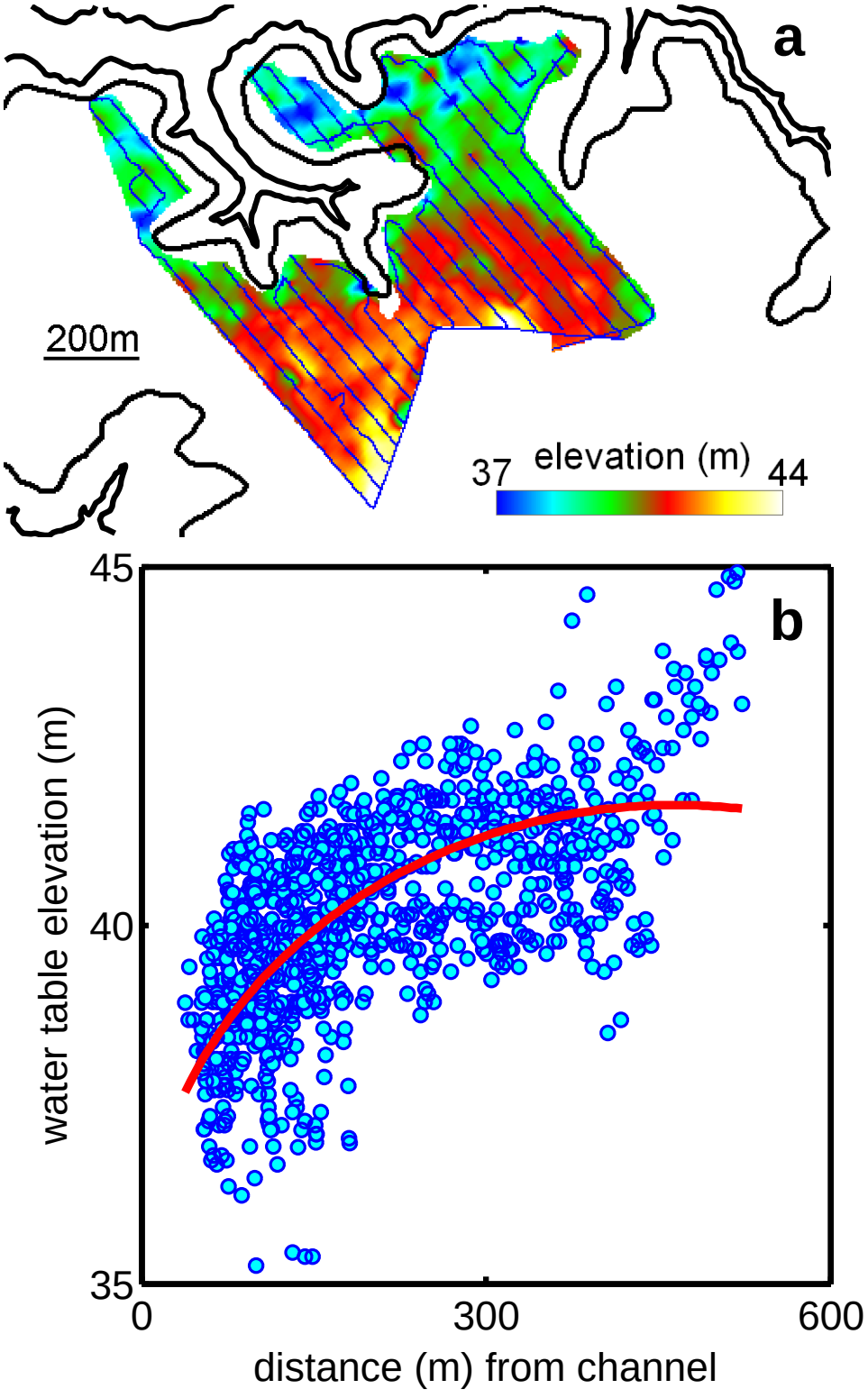
a
200m
37
elevation (m)
44
b
45
40
35
water table elevation (m)
0
300
600
distance (m) from channel

Figure 2

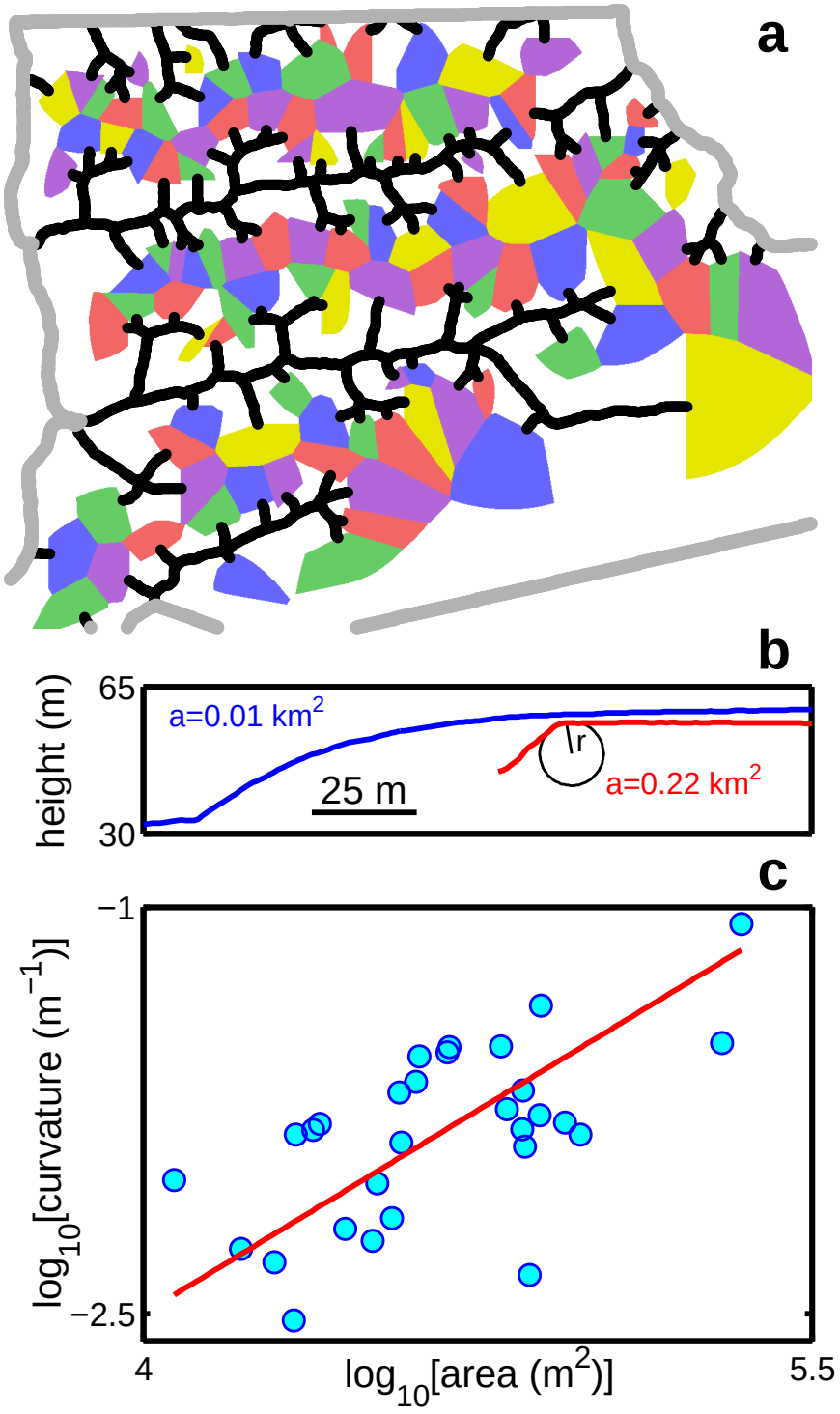
a
b
height (m)
65
30
a=0.01 km2
25 m
r
a=0.22 km2
c
−1
−2.5
log10[curvature (m−1)]
4
5.5
log10[area (m2)]

Figure 3

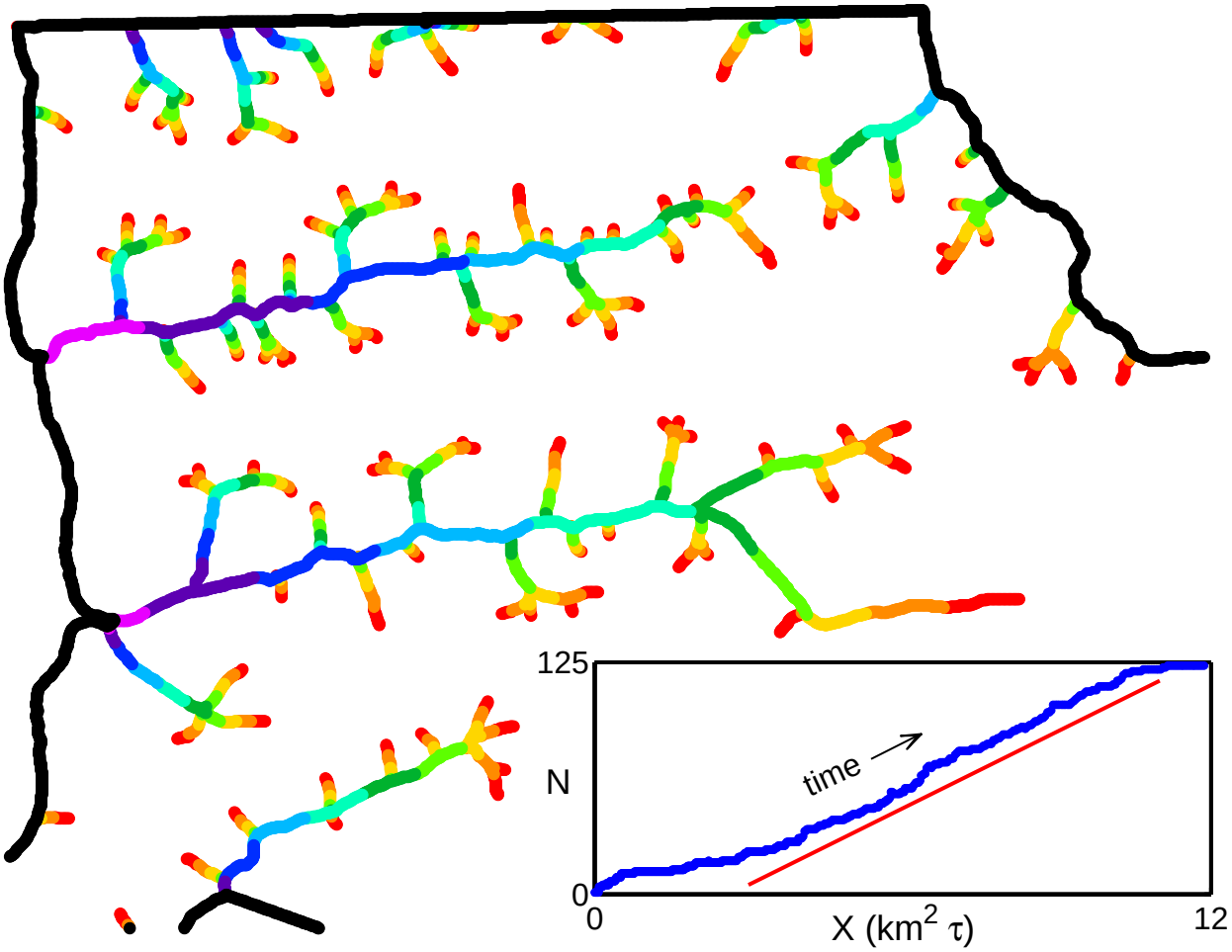

Figure 4